Histol Histopathol (2012) 27: 793-806
DOI: 10.14670/HH-27.793

http://www.hh.um.es

Histology and Histopathology
Cellular and Molecular Biology

Histomorphometrical and proliferative aspects of placenta and uterus of the collared peccary (*Tayassu tajacu*)

Tatiana C. Santos[1], Cristiane Tonarelli[2], Fábio A. Teixeira[2], Moacir F. Oliveira[3], Durvanei Maria[4], Patrícia Reginato[4], Jose R. Kfoury Jr.[2], Carlos A.L. Oliveira[1], Daniela A.L. Lourenço[1] and Maria A. Miglino[2]

[1]Department of Animal Science, State University of Maringá, Maringá, Paraná, Brazil, [2]Department of Surgery, School of Veterinary Medicine, University of São Paulo, São Paulo, Brazil, [3]Department of Animal Science, Federal Rural University of the Semi-Arid. Mossoró, Rio Grande do Norte, Brazil and [4]Butantan Institute, São Paulo SP, Brazil

Summary. The histomorphometric and proliferative characteristics of the collared peccary (*Tayassu tajacu*) placenta and uterus were analyzed. The material was examined by standard histological techniques and histochemistry (PAS, Perls and Alcian Blue pH 0.5 and 2.5%) and the cellular proliferation by AgNORs and flow cytometry. All the analyzed morphometric variables differed between pregnant and non-pregnant uteri in the luteal phase using the Dunnet test. Height and gland diameter of uterine glands increased linearly during pregnancy, with an intense positive PAS and Perls reaction in all stages. The cells with more than seven AgNORs per nuclei and the cells in the G2M cell cycle phase in the maternal tissue also increased after 70 days of pregnancy. The uteroplacental ridges had a linear increase in size with two distinct areas, base and top, with uterine epithelium and trophoblastic cells changing their morphology following the placental ridge development. Flow cytometry analysis showed the percentage of cells in each cell cycle phase with a quadratic behavior for stages G2/M in the maternal tissue, suggesting an increase in proliferative capacity of maternal tissue after 65 days of pregnancy. The same quadratic effect was observed in the G0/G1 phase in both maternal and fetal tissues. Cells in apoptosis showed cubic behavior in both tissues. The morphometric and cellular dynamic aspects observed in this study have not been previously described and they extend our knowledge of functions relating to maternal-fetal dynamics in this species.

Offprint requests to: Dra. Tatiana C. Santos, Department of Animal Science, State University of Maringá Av. Colombo 5790, Maringá, PR 87020-900, Paraná, Brazil. e-mail: tcsantos@uem.br

Key words: Tayassu, Epitheliochorial, Trophoblast, Flow cytometry, AgNOR

Introduction

The *Tayassu tajacu* (collared peccary) is a wild American suidae (Sowls, 1984) and shares its placental morphology with the domestic pig, presenting a chorioallantoic, diffuse, folded and epitheliochorial placenta (Santos et al., 2006). This morphologic similarity to that of other Suidae extends to the molecular level (Corbin et al., 2007). The collared peccary has a gestational period of 144-148 days (Sowls, 1961), and may have one (17.6%), two (79.7%) or three offspring (2.7%) (Mayor et al., 2007), with an average weight of 600 g (Sowls, 1961).

The trophoblast, in the epitheliochorial placenta, adheres to an intact uterine mucosa in order to make maternal-fetal exchanges. In this type of placenta, the placental barrier is complete, theoretically presenting six layers separating the maternal-fetal circulation: maternal endothelium, connective tissue, maternal epithelium, trophoblast, fetal connective tissue and fetal endothelium (Leiser and Kaufmann, 1994; Dantzer, 2002). This disposition can be found in a number of monkeys (Mossman, 1987), horses (Amoroso, 1952), and suiformes (MacDonald and Bosma, 1985), such as Hippopotamus, domestic pigs (Amoroso, 1952) and wild pigs of the genera Sus, Hylochoerus, Babyrousa, Phacochoerus, Chacoan and Tayassu (Macdonald and Fowden, 1997; Benirschke 2000; Santos et al., 2006).

In the suidae placenta, the exchange area increases considerably during pregnancy, both macroscopically and microscopically. In swine (Dantzer, 1999) and

peccaries (Santos et al., 2006) the maternal-fetal contact area increases due to the proliferation of placental ridges, characterizing a folded placenta. The development of both the placenta and the uterus is essential for an adequate supply of nutrients and gases to the fetuses and an increased uterine mass. In cattle, for instance, mass gain can be obtained by cell proliferation or hypertrophy (Boos et al., 2003).

Two methods were chosen to study the proliferative characteristics of the collared peccary placenta, flow cytometry and AgNORs. Nucleolar organizer regions (NORs) are characterized by arrays of rDNA cistrons that usually cluster together to yield one or more nucleoli. In special circumstances (e.g. cancer cells) the NORs may be dispersed inside the nucleus in dot-like structures or altered shapes (Romao-Correa et al., 2005). The number and intensity of silver-stained NORs (AgNORs) are related to the rDNA transcriptional activity and cell proliferation indexes (Derenzini, 2000). The AgNOR procedure has been applied in tumor pathology for both diagnostic and prognostic purposes. Although investigation has been done in trophoblastic tissues in cases of hydropic abortion and hydatidiform moles (Neudeck et al., 1997), there is a paucity of studies involving physiologic tissues.

Multiparameter flow cytometry can be used to assess proliferation and death of cells. The DNA histograms resulting of this analysis represent the number of cells in sub-G1 (apoptosis), G0/G1, S, and G2/M phases of the cell cycle. The G1 phase can be influenced by several external and internal factors. Cells in G1 quiescence may pass the restriction point G1/S and proliferate; conversely, they may undergo senescence in G0 and die (via apoptosis). In contrast to G1, the S, G2 and M phases of the cell cycle are relatively constant in duration. Moreover, cells in G1 comprise the largest fraction of the cycling subpopulation and therefore are the major source of uncertainty in estimations of the growth fraction (Disalvo et al., 1995).

The most commonly used dye for quantification of DNA content and for cell cycle analysis is propidium iodide (PI), which stains whole cells or isolated nuclei. The PI intercalates into the major groove of double-stranded DNA and produces highly fluorescent adducts that can be excited at 488 nm, with a broad emission centered around 600 nm (Vindelov and Christensen, 1990).

Despite the previously mentioned morphological similarities with domestic swine, peccaries represent a unique group of swine, forming part of the American fauna and demonstrating considerable potential for animal husbandry. Notwithstanding the morphological studies already performed, some aspects still need attention in this species, such as the process of implantation, cellular behavior during the first period of pregnancy and the maternal mechanisms of gestation recognition, among others. Thus, this work aims to describe the morphometric characteristics of the main cells involved in maternal-fetal exchanges in collared peccary. In order to achieve this, we analyzed morphometric parameters throughout the collared peccary pregnancy and compared them with non-pregnant uteri in the luteal phase. The relationship between cell proliferation and stage of pregnancy was also studied in the collared peccary placenta.

Materials and methods

Animals

The material necessary for this project was collected in the Center for Wild Animals Multiplication (CEMAS/Ufersa, RN, IBAMA nº 1/24/92/0040-4), in 2004 and 2005, and is registered at IBAMA (nº 2001.003237/05). This research was approved by the Bioethics Committee of the School of Veterinary Medicine of the University of São Paulo (protocol nº17/2002).

Eight animal groups comprising three females (50±25 months) and one male were housed in 2.5x20.0 m pens, with food and water *ad libitum*, for 5 months. After this period, all females were immobilized mechanically and anaesthetized with sodium thiopental (10 mg/kg), and after loss of consciousness and absence of response to stimuli animals were sacrificed by exsanguination of the jugular vein. After euthanasia, uteri were collected and fetuses were euthanatized by cervical dislocation.

The weight of fetuses (Table 1) was used to estimate the age of the pregnancy (in days), based on a formula

Table 1. Female and fetal data from collared peccary. Age of female in months, average of all fetal crown rump (cm) and weight (g), number of fetuses by female, number of *corpus luteum* in both ovaries, and estimated days of pregnancy.

Group	Female (months)	Fetus average (cm)	Fetus average (g)	Number of fetuses	Number of CL	Pregnancy (days)
NP	30.7	-	-	-	1	-
	13.0	-	-	-	3	-
	47.7	-	-	-	1	-
	34.2	-	-	-	2	-
35	88.0	-	-	2	2	> 35
	30.6	-	-	1	3	> 35
	29.6	-	-	1	2	> 35
	43.5	1.2	-	1	2	> 35
75	91.3	7.5	20	1	2	73.1
	90.5	5.8	20	1	3	73.1
	46.2	9.5	45	1	3	75.9
	62.0	9.5	50	1	2	76.5
115	20.4	15.0	235.5	2	2	97.3
	43.5	17.5	292.2	2	2	103.6
	30.9	18.0	396.0	2	2	115.3
	38.0	19.0	410.0	1	1	116.8
135	61.3	23.5	520.5	2	2	129.2
	33.1	22.0	593.0	2	2	137.3
	24.6	22.0	618.0	2	2	140.1
	91.1	25.0	650.0	1	3	143.7

established by Smith and Sowls (1975) (Y=103.78+0.112 (fetal weight - 293.52)). Females with embryos (crown-rump length around 1.0 cm) were considered in groups of 35 days of pregnancy. The females were separated into four pregnant groups (n=16): 35 days (<35 days), 75 days (70 to 80 days), 115 days (90 to 120 days), and 135 days (>125 days), and one non-pregnant group (n=4), females with developed *corpus luteum* (CL) at least in one ovary.

Tissue procedures

Tissue samples from uterus (endometrium and myometrium) and uterus+placenta (chorioallantoic) were immersion fixed in 10% buffered formaldehyde in 0.1 M phosphate buffer, pH 7.3. Tissue samples were also immediately snap-frozen in liquid nitrogen to be used for flow cytometric analysis. The material from the non-pregnant group was obtained from the middle part of the uterine horn, and, in females with just one CL, the material was obtained from the ipsilateral uterine horn.

In pregnant groups, samples were collected from the mesometrial side in one placenta.

Samples were processed by standard histological procedures, embedded in paraplast or in plastic resin (Historesin®, Leica, Germany) and then 5 and 1-μm sections were obtained. Histochemical assays were performed on slides using Perls Prussian Blue reaction, Periodic acid Schiff (PAS) reaction, with and without pretreatment with 1% amylase (Sigma, St Louis, Missouri, U.S.A.) at 98.60°F for 30 min, and Alcian Blue pH 0.5 or 2.5, in order to identify iron, neutral glycoproteins, and mucosubstances, respectively.

Plastic resin slides of 1 μm were stained following Hematoxylin-phloxine and analyzed in morphometric parameters. Measurement was performed in slides, from each female of all groups, with the software Kontron Zeiss 400.3 in an Olympus light microscope. Length and width of uterine gland cells, uterine epithelium and trophoblastic cells were obtained in 200 cells, in 10 different sections, measured by 100x objective. The internal (luminal) and external (including the epithelium) diameter of uterine glands were obtained in 50 transversal cross sections from each female. Muscular tunica (through two muscular layers) and endometrium (from muscular layer to the base of uterine ridge side) thickness were obtained with 10x objective in 50 different areas. Finally, the length of placental ridges was obtained in the placenta after 75 days (base to the top, including uterine epithelium at the base and trophoblast on the top), with a 10x objective in 50 different areas. The average of all parameters was used for statistical analysis.

One-step NOR silver staining

Sections (5 μm thick) were obtained from each paraffin block, deparaffinized in xylene (100%) and ethanol (100 to 70%), post-fixed for 30 min in 3:1 absolute ethanol-acetic acid solution, and rehydrated. For AgNOR staining, two solutions were prepared; the first was gelatin 2% dissolved in aqueous formic acid 1% and the second was 50% aqueous silver nitrate. These two solutions were mixed in a 1:2 ratio and the mixture was immediately poured onto a tissue section (which was left in the dark at room temperature for 20 min). The silver colloid was washed from the sections with distilled, deionized water and the sections were blocked for 1 min with 1% thiosulfate solution (modified from a protocol for placental staining (Ploton et al., 1986)). Slides were washed again, dehydrated through a graded series of ethanol to xylene, and mounted. From the same paraffin blocks, 5 μm sections were stained with Haematoxylin-eosin (HE) to assess tissue morphology. For description and morphology data see previous publication (Santos et al., 2006).

The nuclei of uterine epithelium, uterine glands and trophoblastic cells were analyzed by light microscopy in oil immersion, 200 nuclei/cellular types in 5 randomized fields. The total AgNORs number (dots + clusters) in each nucleus was classified into 3 groups: 1 to 3; 4 to 6; and >7 AgNORs/nucleus. The datam was expressed as a percentage of cells in each group.

Flow cytometry (FACS)–DNA content and cell cycle analysis

Fragments stored in liquid nitrogen were placed into citrate buffer, pH 7.6, and processed according to Vindelov and Christensen (1990). Samples from uterus had myometrium and endometrium and the placenta samples had the chorioallantoic membrane. In brief, samples were filtered through a 30 μm mesh (Spectra Mesh Nylon Filters, Sigma Chemical Co., St. Louis, MO, USA), to be subsequently incubated in 30 mg/mL trypsin (Sigma Chemical Co.) for 10 min, followed by 10 min in 5 mg/mL trypsin inhibitor (Sigma Chemical Co.) and 0.1 mg/mL ribonuclease A (Sigma Chemical Co.), all at RT. Then, 415 μg/mL propidium iodide (Sigma Chemical Co.) was added to the samples 15 min prior to flow cytometric analysis. At least 10,000 events were acquired using Cell Quest Software (Beckton Dickinson, San Jose, CA, USA). DNA content was measured using a FACSCalibur Flow Cytometer (Beckton Dickinson) equipped with an air-coupled 15 mW, 488 nm argon ion laser. The proportion of cells in apoptosis (sub-G1 or DNA fragmentation) or in each phase of the cell cycle (G0/G1, S, G2/M) was calculated using the ModFit Software analysis (Beckton Dickinson). The obtained data was expressed as a percentage of cells in each cell cycle phase.

Statistical analyses

Uterine glands and uterine layer parameters were analyzed using general linear regression by PROC GLM of SAS (2001). A regression model was adjusted to describe the behavior of the variables studied according

to pregnant days and, moreover, the averages of pregnant female groups were compared to non-pregnant in luteal phase using Dunnet test (P<0.05). The female's age was considered in the statistical model as a variation cause in morphometric variables, aiming to reduce residual variation. For uterine epithelium and trophoblasts, data was compared in two separate locations of the maternal-fetal ridges (top and base), after 75 days of pregnancy. Means were compared by Tukey's test (P<0.05).

Concerning cell proliferation data, variance analysis and Tukey's test at a significance level of 5% were performed in order to verify possible variations between cell percentage in each cell cycle phase, throughout pregnancy, covering both maternal and fetal tissues. Differences in the percentage of the AgNOR count, throughout pregnancy, in uterine epithelium, uterine gland epithelium and trophoblasts, were also tested by the same analytical method.

In addition, we proceeded to a regression analysis to study the behavior of cell types throughout pregnancy for each tissue. Through an identity test we verified the difference in behavior of: the same cell type, different tissues and different cell types within the same tissue. Analyses were performed using SAS (2001).

Table 2. Mean and standard deviation of the morphometric thickness of uterine layers of the collared peccary placenta and uterus.

Groups	Myometrium thickness (μm)	Mucosa thickness (μm)	Placental ridge height (μm)
NP	1,060.90±307.04	1,668.60±74.87	-
35	956.28±150.48*	1,101.95±153.45*	-
75	959.86±113.86*	599.71±160.53*	163.75±26.26
115	574.34±63.42*	640.23±64.22*	193.83±30.12
135	863.87±182.83*	647.85±188.18*	307.32±29.29
Effect	ns	Quadratic[1]	Quadratic[2]

*: The mean difference compared to group NP by Dunnet test (P<0.05). NP: non-pregnant; ns: non-significant. [1]y: 2,292.95-34.77x+0.172x^2; R^2: 0.63; [2]y: 814.93-14.83x+0.082x^2; R^2: 0.86

Results

Data from fetuses and females are compiled in Table 1. The observed peccary ovaries presented, in 50% of cases, one or two *corpus luteum* more than the number of fetuses or embryos present inside the uterus. Of the 20 analyzed females, 15% had one, 60% had two and 25% had three *corpus luteum*.

On the maternal side, tissue morphometric data on the thickness of the uterine muscle layer, the external and internal diameter (lumen) of the uterine glands, the height and width of the glandular cells of uterine epithelium and trophoblast cells, in addition to the height of the ridges of the placenta, were analyzed in non-pregnant females and during pregnancy. Data were statistically analyzed and results are shown in Tables 2-4. The female age, in months, or the number of fetuses did not significantly influence the analyzed variables.

Histomorphometric results

In the non-pregnant group, the uterine muscle layer of collared peccaries presented 1,060.90 μm thickness, statistically different from that of the pregnant group, which was approximately 849.06 μm (Table 2).

The endometrium or mucosa was composed of the uterine epithelium and uterine glands scattered in the loose connective tissue. The area of the mucosa with uterine glands presented a difference in thickness (P<0.05) between pregnant and non-pregnant animals, with quadratic behavior decreasing thickness throughout pregnancy with a slight increase towards the end (Table 2).

The histochemical analysis of the glandular activity indicated low activity in non-pregnant females, which had *corpus luteum*, with little PAS+ content in the glandular cytoplasm, when compared qualitatively to those throughout gestation (Fig. 1). Since the initial stages of pregnancy, intense secretory activity was observed and characterized by the presence of cytoplasmic granules, luminal contents and areolar PAS+ content in the uterine glands. Furthermore, the typical

Table 3. Mean and standard deviation of the morphometric data from glandular epithelium and gland diameter (μm) of the collared peccary at different stages of pregnancy and in non-pregnant uterus.

Group	Glandular epithelium		Gland diameter	
	height	width	external	luminal (internal)
NP	18.55±5.74	5.41±0.69	42.36±10.99	9.41±2.52
35	17.03±1.15	5.4±0.16	44.73±1.98	11.04±0.75
75	20.34±2.61	7.19±0.26*	58.74±5.18*	20.36±1.75*
115	23.55±1.99	8.35±0.15*	70.10±2.99*	24.42±1.01*
135	30.31±2.21*	10.79±0.21*	94.18±9.01*	37.33±7.06*
Effect	Linear[1]	Linear[2]	Linear[3]	Linear[4]

*: The mean difference compared to group NP by Dunnet test (P<0.05). NP: non-pregnant; [1]y: 9.498+0.149x; R^2: 0.81; [2]y: 2.615+0.059x; R^2: 0.90; [3]y: 17.73+0.5509x; R^2: 0.85; [4]y: -1.967+0.284x; R^2: 0.81

blue dots from positive Perls reaction inside glandular cytoplasm were observed starting from 45 days of pregnancy. Glandular cells had a negative reaction to Alcian Blue (Fig. 1).

Morphometrically, glandular and luminal diameters were different between pregnant and non-pregnant females, especially when starting from the 75th day of pregnancy (Table 3). The glandular epithelial cells became wider as of this period until the conclusion of the pregnancy (135 days) and also increased in height. The glandular length and width, and also the external and internal glandular diameter, had positive linear behavior throughout pregnancy (Table 3, Fig. 1).

The mucosa of the non-pregnant uterus in collared peccaries is covered by a simple epithelium, the uterine epithelium, composed of columnar cells (25.56x5.83 μm). At the beginning of pregnancy, approximately 45 days, the uterine epithelium changes its format to a low columnar aspect (20.58x12.70 μm) and it is possible to identify the attached fetal membranes (Fig. 2). The

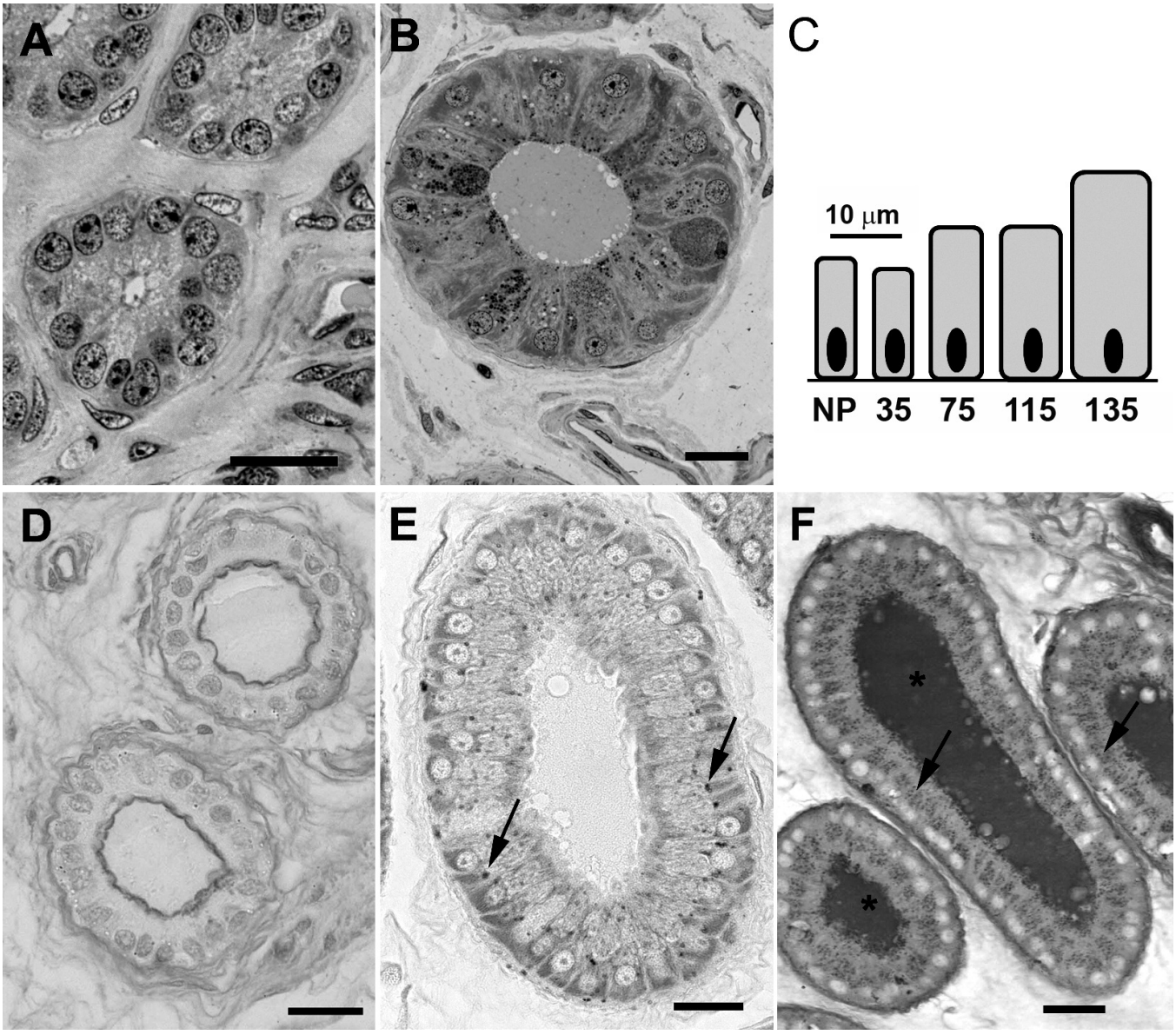

Fig. 1. A-B. Historesin morphological aspects of the uterine glands in non-pregnant **(A)** and pregnant collared peccaries **(B)**. Note the cytoplasmic granules **(B)**. Historesin, Harris Hematoxylin. **C.** Schematic diagram based on weight and length obtained in each period in histological sections of uterine glands. **D-F.** Histochemistry of uterine glands demonstrating a negative reaction to Alcian blue, positive dots to Perls reaction (arrows), and positive PAS reaction on cytoplasmic granules (arrow) and lumen (*). Scale bars: 20 μm

uterine epithelium presented significant differences in height and width between pregnant and non-pregnant animals (Table 4).

At 35 days of pregnancy trophoblastic cells were columnar (41.25x10.14 μm) with evidence of a thin layer of mesenchyme and fetal vessels. At this stage it is already feasible to observe the formation of areolae characterized by areas in which there is a distance between uterine epithelium and trophoblast, with eosinophilic secretion and PAS+ in the space formed (not shown).

After this period, the maternal-fetal interface begins to bend, forming maternal-fetal ridges. These ridges can be witnessed as smooth curves which increase in complexity and height throughout the pregnancy with quadratic behavior (Table 2). Fetal ridges also change their shape in areolae throughout pregnancy, becoming ever more complex, but these were not analyzed. The morphological aspect of the uterine epithelial and trophoblastic cells was influenced by the position on these maternal-fetal ridges and morphometric results are expressed in Table 4. After 75 days, when a morphologic difference among cells in both regions was present, results were compared in both regions of ridges, base and top.

The uterine epithelium cells became irregularly flat throughout gestation, especially at the base of the maternal ridges, 10.24±1.46 μm and 19.56±3.85 μm in

Table 4. Mean and standard deviation of the morphometric height and width of uterine epithelium and trophoblast of the collared peccary at different stages of pregnancy and in non-pregnant uterus.

Days of pregnancy	Cellular measurement			
	height	width	height	width
Uterine epithelium				
NP	25.56±8.26	5.83±1.19		
35	20.58±2.81	12.70±1.11		
	Top of materno-fetal ridge		*Base of materno-fetal ridge*	
75	18.97±1.45	13.64±1.68	11.17±1.52	17.02±1.35[a]
115	15.75±2.27	12.26±0.28	9.77±1.93	18.09±3.46[a]
135	15.28±0.71	12.86±1.52	9.67±0.71	23.22±3.32[b]
Average	**16.75±2.22**	**12.98±1.37**	**10.24±1.46**	**19.56±3.85**
Trophoblast				
35	41.25±3.19	10.14±0.70		
	Top of materno-fetal ridge		*Base of materno-fetal ridge*	
75	45.59±3.03	9.45±1.19	21.78±2.46	13.39±1.73
115	43.44±5.59	9.40±0.59	25.05±1.90	14.24±1.45
135	37.89±2.99	9.40±0.92	22.13±1.90	16.05±1.90
Average	**42.20±4.91**	**9.41±0.87**	**22.81±2.40**	**14.59±1.97**

[a-c]: Values (means) in the same row with different superscripts differ by Tukey test (P<0.05); NP: non-pregnant.

Table 5. Distribution of the AgNOR quantity (in %) in placental cells of collared peccary at different stages of pregnancy and in-non pregnant uterus.

Number of AgNORs	NP	Days of pregnancy				Effect	SEM
		35	75	115	135		
	Uterine epithelium						
1 to 3	27.25[B]	50.75[A]	33.50	49.13[A]	44.13[A]	ns	5.42
4 to 6	54.50[A]	45.88[A]	44.00	44.25[A]	46.63[A]	ns	5.42
>7	18.25[B,ab]	03.38[B,c]	22.50[a]	06.63[B,bc]	09.25[B,abc]	ns	5.42
	Glandular epithelium						
1 to 3	29.63[B,b]	58.75[A,a]	58.38[A,a]	51.38[A,ab]	34.25[AB,ab]	Quadratic	4.87
4 to 6	56.25[A,a]	39.63[A,ab]	34.75[A,b]	42.75[A,ab]	54.00[A,ab]	Quadratic	4.87
>7	14.13[B]	01.63[B]	06.88[B]	05.88[B]	11.75[B]	Quadratic	4.87
	Trophoblast						
1 to 3	-	50.38	34.00	40.75	35.50	ns	5.08
4 to 6	-	43.88	44.50	47.50	48.25	ns	5.08
>7	-	05.75	21.50	11.75	16.25	Cubic	5.08

SEM: standard error medium; NP: non-pregnant; ns: non-significant; [A-B]: Values (means) in the same column with different superscripts differ (P<0.05); [a-c]: Values (means) in the same row with different superscripts differ (P<0.05); ns: (P>0.05).

height and width, respectively, and conserved the cuboidal form, and 16.75±2.22 and 12.98±1.37 μm in height and width, respectively, on the top of ridge (Table 4, Fig. 2). Trophoblastic cells were cylindrical with 42.20±4.91 μm in height and 9.41±0.87 μm in width at the top. Trophoblastic cells presented cuboidal shape on the base of the fetal ridges after 75 days of pregnancy with 22.81±2.4 μm in height and 14.59±1.97 μm in width (Table 4, Fig. 2).

The uterine epithelium cells had secretory activity throughout the entire pregnancy, revealing cytoplasmic granules whose PAS+ secretion could be observed in the maternal-fetal interface (Fig. 3). The trophoblast presented PAS+ granules in the basal pole of cells in the fetal side.

The trophoblast was supported by the mesenchyme, made by loose connective tissue and full of blood vessels. The mesenchyme had an intense positive

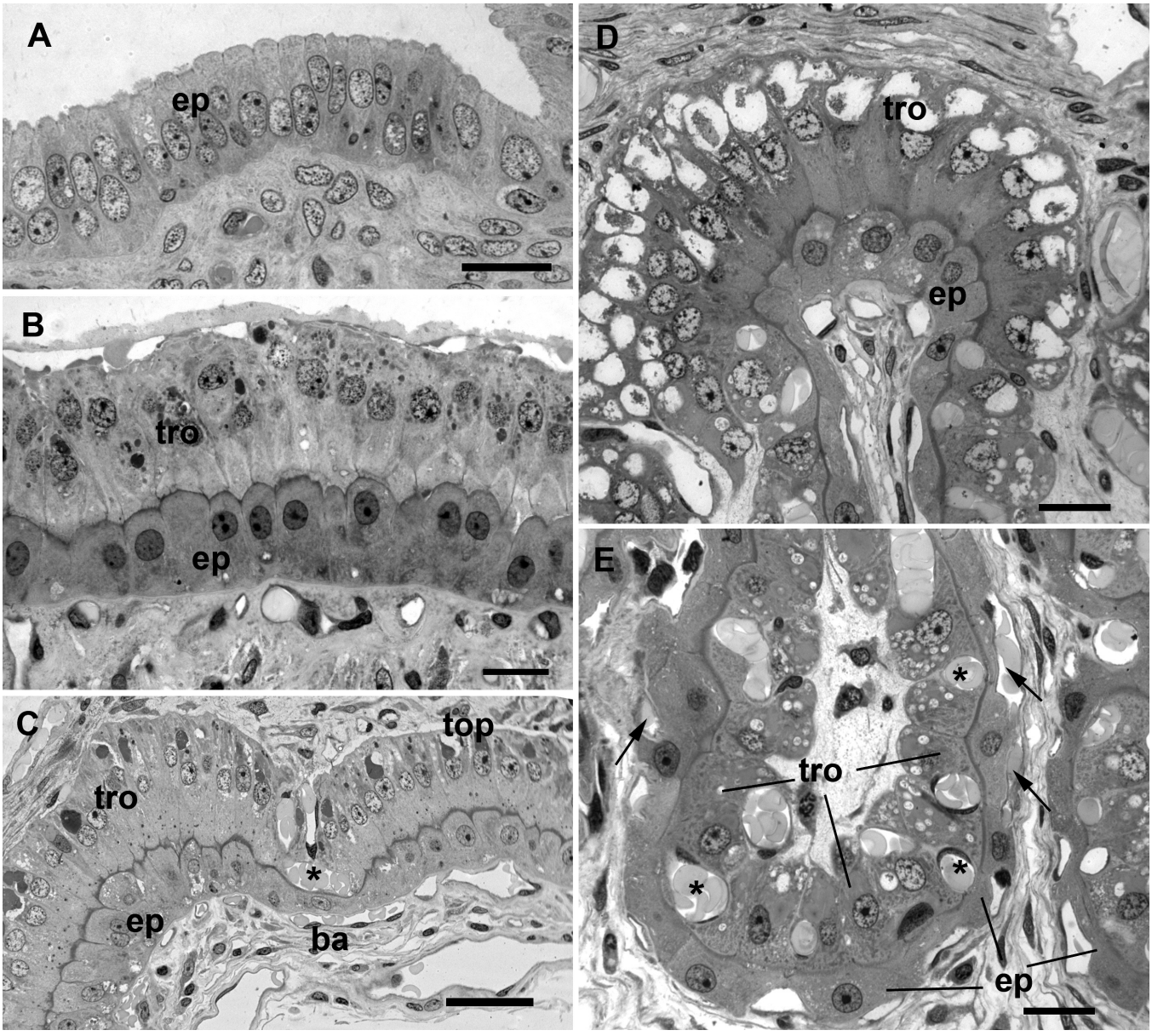

Fig. 2. Uterine epithelium (ep) and trophoblast (tro) morphology through pregnancy in collared peccary. **A.** Columnar uterine epithelium in a non-pregnant female. **B.** Trophoblast with columnar aspect in connection with uterine epithelium at approximately 35 days of pregnancy. **C.** Formation of placental folds with commencement of morphological differentiation at base (ba) and at top (to) of placental fold at 75 days. **D-E.** Distinct morphological differentiation of the trophoblast and uterine epithelium between top **(D)** and base **(E)** of placental folds at middle and late pregnancy. Fetal capillaries (*). Historesin, Hematoxylin floxin, Scale bars: A-B, D-E, 20 μm; C, 60 μm

reaction to Alcian blue (pH 2.5), primarily inside the placental ridges and in one band on the base of the fetal ridges (Fig. 3). The connective tissue did not react to Alcian Blue stain and was PAS+, especially around uterine glands (Fig. 1F).

AgNORs and flow cytometry results

The ability of cells to proliferate was evaluated by intranuclear AgNOR count (one-step silver staining NOR) and by flow cytometry in the empty uterus of females in the luteal phase, and in the placenta of collared peccary, throughout pregnancy. The AgNOR count allowed an inference for each specific cell type. The uterine epithelium, the trophoblast and the uterine gland epithelium were analyzed by said method, while cell pools in the mucosa on the maternal side, and in the chorioallantoic membrane on the fetal side, were

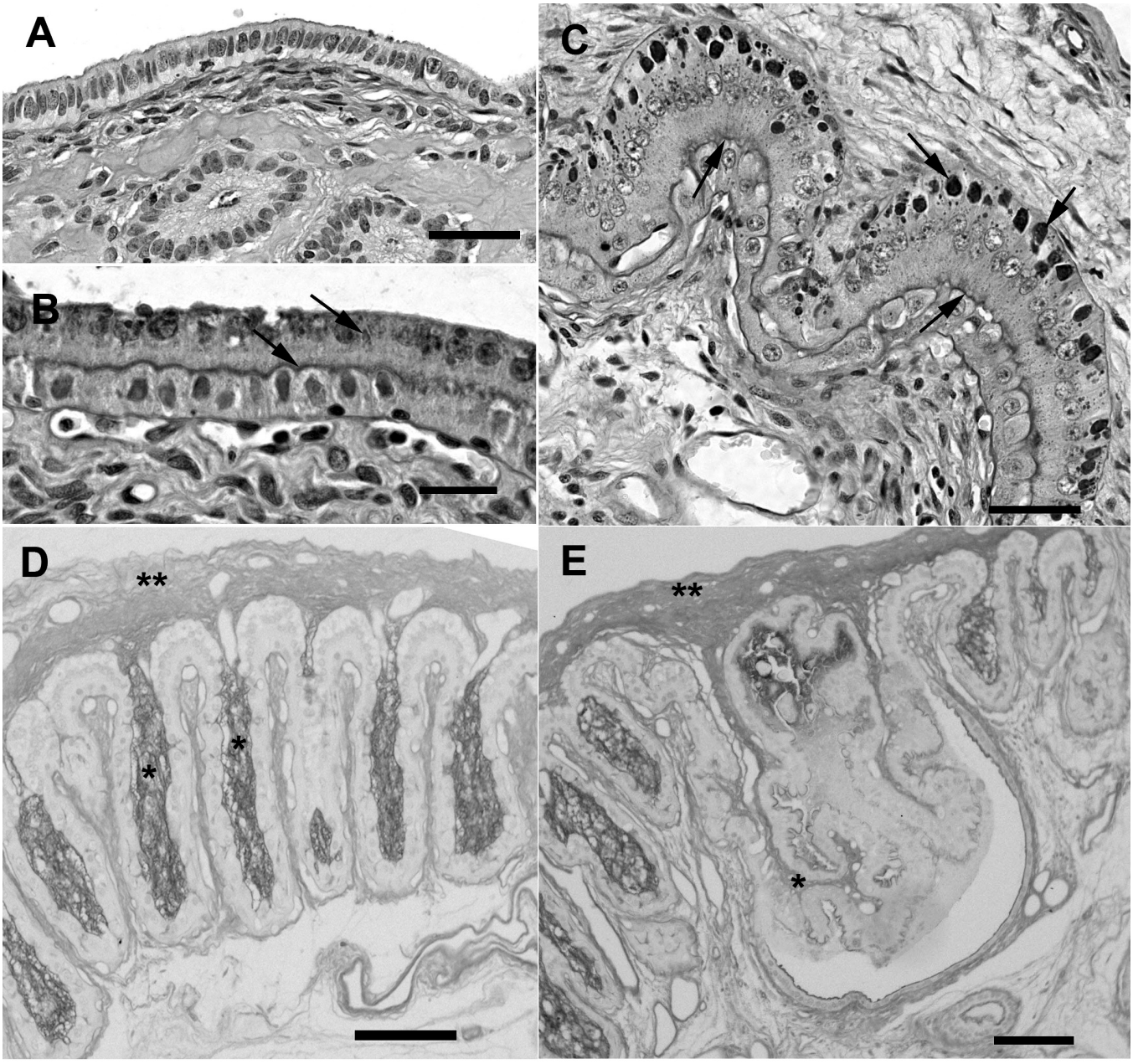

Fig. 3. Histochemistry of the placenta of collared peccary. **A-C.** Histochemistry in the beginning **(A),** 45 **(B)** and 75 days **(C)** to PAS. Positive reaction in the maternal-fetal interface (arrows) and in cytoplasmic granules of trophoblast (arrows). **D-E.** Alcian Blue pH 2.5 reaction + for carboxylated acidic glycosaminoglycans in a band of mesenchyme at base (**) and filling the fetal folds (*). Scale bars: A-C, 20 μm; D-E, 100 μm

analyzed by flow cytometry. When analyzed through AgNOR count, cells had, in general, between one and three clusters/cell types, while the number of dots varied, reaching beyond 10 dots/nucleus (Fig. 4). The number of AgNORs was considered the sum of Dots and Clusters in each cell type.

No significant abnormalities among cell groups having up to six AgNORs per nucleus existed in regards to the uterine epithelium cells. Cells with more than seven AgNORs per nucleus were significantly higher in non-pregnant uterus and at 75 and 135 days of pregnancy (Table 5).

The uterine epithelial cells indicated no significant variation relating to the number of intranuclear

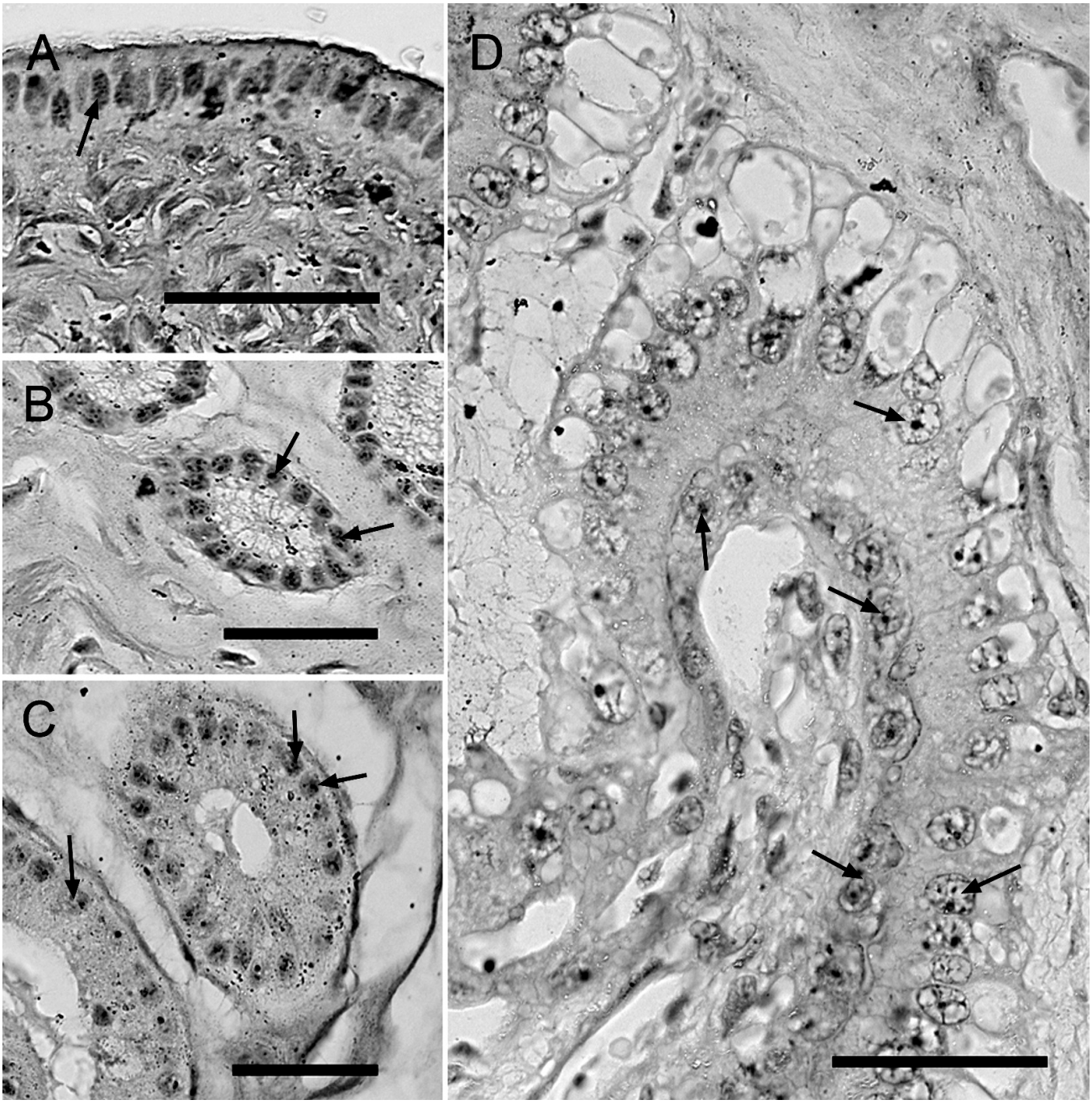

Fig. 4. AgNORs in cellular nuclei (arrows) of uterine epithelium and endometrial glands of non-pregnant collared peccary **(A-B)** and in late gestation **(C-D)**. Scale bars: 40 μm

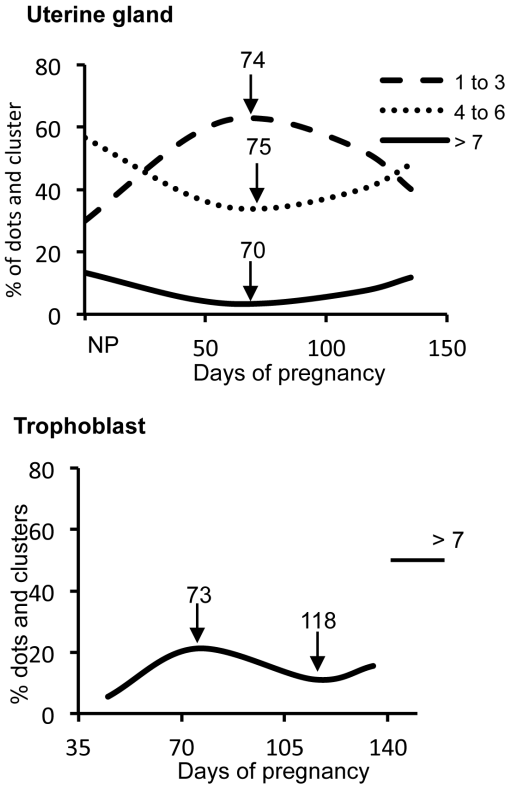

Fig. 5. Significant regression curves of the AgNORs distribution (%) in glandular epithelium and trophoblast in collared peccary placenta. Uterine glands: One to three AgNORs $Y=29.879+0.886X-0.006X^2$; $R^2=0.98$; 4 to 6 AgNORs $Y=56.716-0.604X+0.004X^2$; $R^2=0.99$, and >7 AgNORs $Y=13.405-0.282X+0.002X^2$; $R^2=0.75$. Trophoblast: >7 AgNORs $Y= -137.2+5.47X-0.0606X^2+0.00021X^3$; $R^2=1.00$

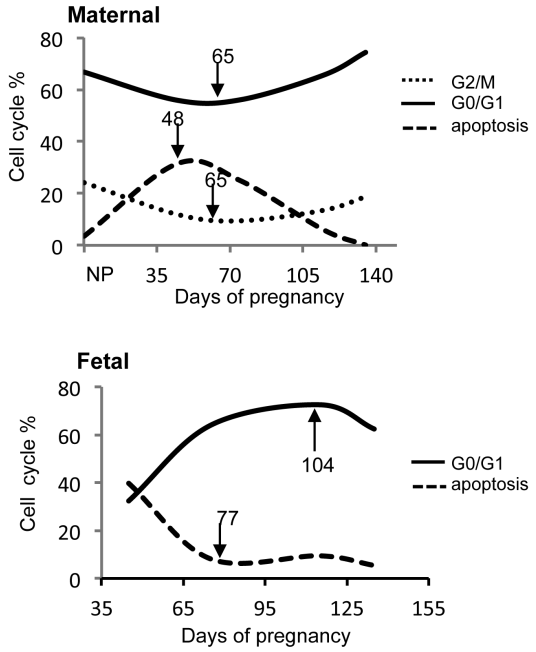

Fig. 6. Significant regression curves of the percentage of cells in different cell cycles (G2/M, G0/G1, and apoptosis) from maternal and fetal tissue in collared peccary placenta and uterus, after Flow Cytometry procedures. Maternal tissue: G2/M $Y=24.22 - 0.393X+0.0027X^2$; $R^2=0.53$; G0/G1 $Y=66.66-0.389X+0.0033X^2$; $R^2=0.95$; and Apoptosis $Y=3.54+1.350X-0.019X^2+0.00007X^3$; $R^2=0.94$. Fetal tissue: G0/G1 $Y= -55.55+2.494X-0.012X^2$; $R^2=0.99$; and Apoptosis $Y=223.50-6.627X+0.066X^2-0.0002X^3$; $R^2=1.00$.

Table 6. Distribution of the cell cycle phase variations (apoptosis, G0/G1, S and G2/M) (in %) of the maternal and fetal tissue of the collared peccary at different stages of pregnancy and in non-pregnant uterus.

	Apoptosis	G0/G1	S	G2/M
Maternal tissue				
NP	04.14^{b}	65.54	03.90^{b}	26.68
35	28.80^{a}	58.57	05.66^{ab}	07.38
75	29.63^{a}	55.38	05.25^{ab}	10.18
115	03.47^{b}	64.77	09.69^{a}	22.46
135	02.81^{b}	77.64	04.54^{ab}	15.23
SEM	03.39	05.80	02.46	04.94
Means	**12.49±3.40^{B}**	**59.32±3.40^{A}**	**9.07±3.40^{B}**	**19.36±3.40^{B}**
Effect	Cubic	Quadratic	ns	Quadratic
Fetal tissue				
35	39.48^{a}	32.60^{b}	08.68	19.77
75	07.28^{b}	63.35^{a}	11.95	17.80
115	07.38^{b}	72.95^{a}	07.09	12.29
135	02.56^{b}	61.70^{a}	08.45	27.68
SEM	03.39	05.80	02.46	04.94
Means	**16.18±2.62^{BC}**	**64.09±2.62^{A}**	**6.28±2.62^{C}**	**13.81±2.62^{B}**
Effect	Cubic	Quadratic	ns	ns

SEM: standard error medium; NP: non-pregnant; ns: non-significant; $^{A-C}$: Values (means ± SEM) in the same row with different superscripts differ ($P<0.05$); $^{a-c}$: Values (means ± SEM) in the same column with different superscripts differ ($P<0.05$).

AgNORs. A predominance of cells possessing one to three AgNORs and four to six AgNORs was observed in much of the pregnancy. The quantity of cells having greater than seven AgNORs per nucleus was significantly higher at 75 and 135 days of pregnancy, and in non-pregnant uterus (Table 5).

The glandular epithelium demonstrated quadratic behavior for all AgNOR groups. Cell percentage of uterine glands possessing one to three AgNORs had a quadratic behavior ($y=29.879+0.886x-0.006x^2$; $R^2=0.98$), increasing up to 74 days, and consequently decreasing from that period on. Cells with four to six AgNORs ($y=56.716-0.604x+0.004x^2$; $R^2=0.99$) had their percentage reduced until 75 days, when it then increased towards the end of pregnancy. Cell percentage with seven AgNORs ($y=13.405-0.282x+0.002x^2$; $R^2=0.75$) decreased to 70 days of pregnancy, increasing towards the end of pregnancy (Table 5, Fig. 5).

A predominance of cells containing one to three AgNORs per nucleus at 45 days and 75 days of pregnancy in the uterine gland epithelium was observed. At 115 days of pregnancy, the quantity of the referred cells decreases and is followed by an increased quantity of cells having four to six AgNORs per nucleus. At 135 days the number of cells possessing four to six AgNORs per nucleus becomes greater still, with an increase in cells comprising more than seven AgNORs per nucleus.

Trophoblastic cells had no statistical variations between the AgNOR groups when ranked by number of AgNORs, but the group having more than seven AgNORs demonstrated cubic behavior ($y= -137.2+5.47x-0.0606x^2+0.00021x^3$; $R^2=1.00$), up to 74 days, decreasing until 118 days and increasing once again from that period on (Table 5, Fig. 5). When averages covering the entire pregnancy were analyzed, trophoblast indicated 46.48%, 40.16% and 13.84% of the cells having one to three, four to six, and greater than seven AgNORs, respectively.

Data analysis by flow cytometry in the maternal tissue (Table 6, Fig. 6) demonstrated a quadratic behavior ($P<0.05$) concerning G2/M phases in the maternal tissue, and G0/G1 phase in both maternal and fetal tissues. Cells undergoing apoptosis, however, exposed a cubic behavior in both tissues.

The quiescent cells in G0/G1 decreased until 75 days in the maternal tissue and increased at the end of pregnancy. In the fetal tissue, the percentage of quiescent cells increased up until 115 days, decreasing towards the culmination of the pregnancy (Table 6, Fig. 6). Cells within the proliferation phase (G2/M) exhibited a significant effect on the maternal tissue, reducing cell percentage in this phase of cell cycle until 65 days, and again increasing towards the end of pregnancy. In fetal tissue, cells maintained an average of 13.81% of cells in G2/M, hence, there was no significant fluctuation between the groups (Table 6, Fig. 6). The percentage of cells in the S-phase of the cell cycle did not alter significantly, averaging 9.7% in the maternal tissue and 6.28% in the fetal tissue. The maternal tissue produced the highest percentage of cells in the S-phase at 115 days of pregnancy (9.69%). However, when comparing the models for each cell cycle phase, the percentage of identified cells in G2/M, S and apoptosis were similar.

Where rates of apoptosis are concerned, the uterine wall cells exhibited cubic behavior ($P<0.05$), increasing until 75 days of gestation, and subsequently decreasing after that period. Fetal tissue progressively decreased in percentage of apoptotic cells until the end of pregnancy (Table 6, Fig. 6). When the models for each cell cycle per analyzed tissue in the flow cytometer were tested, we found that cells in G0/G1 were predominant in the maternal and fetal tissues, although the quantity of cells in other phases of the cell cycle varied. Large variations occur throughout pregnancy, especially between the number of cells in the proliferative G2/M-phase and the number of cells during apoptosis.

Discussion

It is the first time the behavior of cellular metric data of an epitheliochorial placenta has been described throughout pregnancy, and the data obtained compared to that sourced from empty uteri in the luteal phase. The results complemented descriptions previously performed in collared peccary and peccary (Jones et al., 2004; Santos et al., 2006) and added data about cellular dynamics in the placenta of suiforms in general.

Peccaries are wild animals, yet there is a potential occurrence of zootechnical exploration. Despite the heterogeneity in the females in this study, the analyzed variables are representative - the data have coefficients of acceptable variation. The obtained standard error also supports this statement. Notwithstanding the disparity in the age of females and lack of historical reproduction, it was possible to obtain morphometric data representative of the species in question. The data described within this study is essential for possible comparisons between wild and domestic swine and for comparative morphology in general.

In this study, fetuses were approximately 333 g in weight and 17.5 cm crown rump length at 115 days of pregnancy. At the advent of birth, they weighed 595.4 g and their crown rump length was 23 cm, suggesting that the placenta had to work at a quick enough pace to provide the nutrients necessary for considerable fetal development to occur within this 30-day period. This explains the continuous development observed in the uterine glands until the end of pregnancy, together with the development and complexity of the observed placental ridges. The difference observed between number of fetuses and number of *corpus luteum* is explained by embryonic mortality, also reported in peccaries (Smith and Sowls, 1975; Barbella, 1993).

The morphometric data from gland cells and glandular diameter indicate hypertrophy and high activity, suggesting a considerable increase in glandular area, based on the crescent linear behavior of all variables analyzed. In pigs, uterine glands reach their

maximum development near the middle of pregnancy with 48.5 μm, reducing in size to 35.0μm at the end of pregnancy, and to 27.0μm 24 hours after birth (Perry and Crombie, 1982), although in this case the authors committed solely to qualitative analyses. At 75 days, the uterine gland cells in the collared peccaries reached an average height of 20.34 μm, and when nearing delivery (135 days) the height of cells measured 30.31 μm. The biggest glandular diameter and height of cells was observed at 135 days of pregnancy. At the same period, the largest number of cells having more than seven AgNORs/nucleus was noted. These results suggest that increased gland size was followed by an increase in the proliferative aspects of nuclei cells and uterine glands, responding to the proliferation of cells, in number and height.

All mammals contain endometrial glands that synthesize and secrete substances essential for survival and development of the conceptus (Spencer and Bazer, 2004). Particularly in pigs, the pre-implantation period is long and it results in an embryonic dependence of uterine glandular secretion (Gray et al., 2001). The secretory activity of the endometrium in pigs is intense and has vital importance: one of its main functions is to provide iron for the developing embryo (Dantzer, 1984). Iron is secreted in the form of uteroferrin by endometrial glands and absorbed in the areola-gland subunit (Friess et al., 1981; Raub et al., 1985), used for hematopoiesis by the fetal liver and stocked into the allantoic fluid (Renegar et al., 1982).

A positive Perls reaction was observed in the uterus of collared peccaries in all pregnant groups in uterine glands. In female pigs, uterine glands are simple and relatively sparse in those which are non-pregnant, yet throughout pregnancy they become intimately associated with the areolae, forming the functional complex gland-areola in the placenta (Perry and Crombie, 1982, Sinowatz and Friess, 1983). During the final third of pregnancy, glandular secretion remains high and, after parturition, undergoes rapid involution (Perry and Crombie, 1982).

The proliferative capacity of uterine gland cells was confirmed by the AgNOR count in their cellular nuclei. The glandular epithelium demonstrated a tendency to increase the number of AgNORs in cell nuclei with the advancing pregnancy. Cell quantity having one to three AgNORs decreased throughout gestation, while the number of cells showing four to six AgNORs reached its maximum at 135 days of pregnancy. Data suggest a direct relationship between increased cell proliferation and increased diameter of the uterine gland, relating to the intense secretory activity of said structures. Peaks of uteroferrin secretion are cited in swine placenta at the maternal fetal recognition period, around 30 and 60 days of pregnancy (Geisert et al., 1982; Zavy et al., 1984).

The peak of apoptosis in maternal tissues occurred at 48 days, characterizing an intense tissue remodeling taking place in the uterus (early stages of pregnancy). From this period on, the maternal-fetal ridge formation and increased uterine tridimensional complexity, in addition to increased fetal weight, demanded the proliferation of the uterine tissue, observed by the percentage of cells in G2/M, which increased from 65 days of pregnancy until conclusion. This proliferation likely occurred due to the glandular tissue, whose AgNOR count suggests a similar behavior to that observed by flow cytometry.

The emergence of the maternal-fetal ridge around 75 days of pregnancy in the placenta determined the formation of distinct morphological and functional areas at top and bottom. This formation was described in swine (Dantzer, 1999), and in collared and white-lipped peccaries (Santos et al., 2006), although in this study it was possible to determine the morphometric behavior of cells involved in the placental barrier since the beginning of pregnancy.

The adaptations of the cells of both the uterus and placenta are necessary to create some areas specialized in histotrophic exchange (top ridges) and others in gas exchange (base). In the epitheliochorial placenta, throughout gestation, the endometrium has to undergo a phase of growth and remodeling to increase the surface area of exchange, which tends to be highly vascularized. The placenta has to rapidly develop to acquire the capacity to perform like respiratory, intestinal and endocrine systems. The physical distance between the maternal and fetal blood in the interhemal membrane also has to reduce to facilitate the exchanges, especially that of oxygen and carbon dioxide (Dantzer et al., 1988; Leiser et al., 1998). In collared peccary the maternal-fetal ridges increased significantly, but the increase in area because of the branch of the ridges and their complexity was not considered in this study. Variations from 191 μm at 45 days to 361μm at 105 days in the height of placental ridges were observed in pigs (Vallet and Freking, 2007).

The increased height of the fetal ridges promotes an increase in the maternal-fetal contact surface area, especially in lateral areas in which a decrease in the thickness of the interhemal barrier in pigs is mentioned and is what allows an exchange between mother and fetus (Friess et al., 1980). The analyzed material also presented longer ridges towards the end of pregnancy, increasing the area in which capillaries are indented in the trophoblast and uterine epithelium, corresponding to the lateral and top of chorionic ridges (basis of placental ridge). Thus, the placental barrier in collared peccary can reach 3 μm or less (Santos et al., 2006), aiming to facilitate gas exchanges and the transfer of diffusible substances among the tissues (Dantzer et al., 1988; Leiser and Dantzer, 1988).

In fetal tissue we observed the opposite behavior, with the highest apoptosis rates in tissues occurring in early pregnancy. The high percentage of cells undergoing apoptosis at 45 days of pregnancy is related to the increased remodeling tissue in the trophoblast, since, during this period, a few quiescent cells (G0/G1 phase) were observed, demonstrating that they had

engaged in apoptosis. This is confirmed with the observation of a number of cells containing more than seven AgNORs per nucleus at 45 days of pregnancy, showing a low proliferation in the trophoblast during early pregnancy.

The greatest number of proliferating cells in the fetal tissue was observed at 135 days of pregnancy, corresponding to the period having a low apoptosis rate, indicating higher proliferative activity in late pregnancy. Trophoblast cells demonstrated peaks of more than seven AgNORs per nucleus, corresponding to the peak of cells in the synthesis phase (S phase) and in the proliferation phase itself (G2/M phase). This data reveals a strict correlation between techniques, relating the average number of AgNORs per nucleus not only to the proliferative phase of the cell cycle, but also to the synthesis phase of genetic material, as previously observed by Belotti et al. (1997).

Increased apoptosis in females until 75 days of pregnancy both in placental and uterine tissues likely represents the intense remodeling tissue occurring on both sides of the peccary placenta, enabling the formation of maternal-fetal ridges that arrange themselves three-dimensionally to meet the metabolic needs of fetuses.

Apoptosis is apparently important in the final stages of pregnancy on which placental expulsion appears to depend. For example, this is the case of synepitheliochorial placenta of bovine (Boss et al., 2003; Facciotti et al., 2009; Rici et al., 2009). Although animals in this study were not in the parturition stage, this does not appear to be the case for the epitheliochorial placentae, since placental expulsion is physically easier, and vascular pressure alterations within the maternal-fetal ridges seem to be the prime factor for placental expulsion. The connective tissue network supporting blood vessels within these ridges had a key role in maintaining this architecture.

In relation to the placenta at the base of the chorionic ridge or the top of the placental side, the trophoblastic cells maintained their long cylindrical shape throughout the pregnancy, while the uterine epithelium reduced in height until the end of pregnancy. This placental area is responsible for absorbing less diffusible substances, secreted by the cuboidal uterine epithelium (Fries et al., 1980; Dantzer et al., 1981). Another feature that develops and interferes with placental morphology is the indentation of capillaries, aiming to decrease the distance between maternal and fetal blood, to allow for gas exchange between the two liquids. This characteristic is typical of the epitheliochorial type of placenta (Leiser et al., 1998).

In summary, it was possible to demonstrate the morphological changes in placental cells throughout pregnancy in the collared peccary. Peccaries are the most distant relatives of domestic pigs in the Suiform sub-order. Despite millions of years of evolutionary isolation, this wild pig still shares similarities in placental morphology with domestic pigs and these have been previously described and were emphasized by this histomorphometric and cell cycle analysis throughout pregnancy.

Acknowledgements. This study was supported by Fundação de Amparo a Pesquisa do Estado de São Paulo (FAPESP). The authors wish to thank the Wild Animal Multiplication Center from UFERSA for the animals.

References

Amoroso E.C. (1952). Placentation In: Marshall's physiology of reproduction. Third ed. Vol. II. Parkesed A. (ed). Longman, Green and Co. London. pp 127-311.

Barbella S.L. (1993). Gestación y reproducción post-parto en el báquiro de collar (*Tayassu tajacu*). Rev. Fac. Agron. (Maracay) 19, 165-184.

Bellotti M., Elsner B., Kahn A., Bezodnick L., Pisilli L. and Greco P. (1997). Morphometric determination of AgNORs in breast carcinoma. Correlation with flow cytometry and proliferating cell nuclear antigen. Anal. Quant. Cytol. Histol. 19, 139-414.

Benirschke K. (2000). Anatomic studies on pregnant giant peccaries (*Catagonus wagneri*). Zoologic. Garten 70, 201-210.

Boos A., Janssen V. and Mulling C. (2003). Proliferation and apoptosis in bovine placentomes during pregnancy and around induced and spontaneous parturition as well as in cows retaining the fetal membranes. Reproduction 126, 469-480.

Corbin C.J., Hughes A.L., Heffelfinger J.R., Berger T., Waltzek T.B., Roser J.F., Santos T.C., Miglino M.A., Oliveira M.F., Braga F.C., Meirelles F.V. and Conley A.J. (2007). Evolution of suiform aromatases: ancestral duplication with conservation of tissue-specific expression in the collared peccary (*Pecari tayassu*). J. Mol. Evol. 65, 403-412.

Dantzer V. (1984). Intracellular pathway of native iron in the maternal part of the porcine placenta. Eur. J. Cell Biol. 34, 103-109.

Dantzer V. (1999). Epitheliochorial placentation. In: Encyclopedia of reproduction. Vol. 2. pp 18-28.

Dantzer V. (2002). Endometrium of epitheliochorial and endotheliochorial placentae. In: The endometrium. Glasser S.R., Aplin J.D., Giudice L.C. and Tabibzadeh S. (eds). Taylor e Francis. London.

Dantzer V., Bjorkman N. and Hasselager E. (1981). An electron microscopic study of histiotrophe in the interareolar part of the porcine placenta. Placenta 2, 19-28.

Dantzer V., Leiser R., Kaufmann P. and Luckhardt M. (1988). Comparative morphological aspects of placental vascularization. Troph. Res. 3, 221-244.

Derenzini M. (2000). The AgNORs. Micron 31, 117-120.

Disalvo C.V., Zhang D. and Jacobberger J.W. (1995). Regulation of NIH-3T3 cell G1 phase transit by serum during exponential growth. Cell Prolif. 28, 511-524.

Facciotti P.R., Rici R.E.G., Maria D.A., Bertolini M., Ambrósio C.E. and Miglino M.A. (2009). Patterns of cell proliferation and apoptosis by topographic region in normal *Bos taurus* vs. *Bos indicus* crossbreeds bovine placentae during pregnancy. Reprod. Biol. Endocrinol. 7, 1-7.

Friess A.E., Sinowatz F., Skolek-Winnisch R. and Träutner W. (1980). The placenta of the pig. I. Fine structural changes of the placental barrier during pregnancy. Anat. Embryol. 158, 179-191.

Friess A.E., Sinowatz F., Skolek-Winnisch R. and Träutner W. (1981). The placenta of the pig. II. The ultrastructure of the areolae. Anat. Embriol. 163, 43-53.

Geisert R.D., Renegar R.H., Thatcher W.W., Roberts R.M. and Bazer F.W. (1982). Establishment of pregnancy in the pig: I. Interrelationships between preimplantation development of the pig blastocyst and uterine endometrial secretions. Biol. Reprod. 27, 925-939.

Gray C.A., Bartol F.F., Tarleton B.J., Wiley A.A., Johnson G.A., Bazer F.W. and Spencer T.E. (2001). Developmental biology of uterine glands. Biol. Reprod. 65, 1311-1323.

Jones C.J.P., Santos T.C., Abd-Elnaeim M., Dantzer V. and Miglino M.A. (2004). Placental glycosylation in peccary species and its relation to that of swine and dromedary. Placenta 25, 649-657.

Leiser R. and Dantzer V. (1988). Structural and functional aspects of porcine placenta microvasculature. Anat. Embryol. 177, 409-419.

Leiser R. and Kaufmann P. (1994). Placental structure: in a comparative aspect. Exp. Clin. Endocrinol. 102, 122-134.

Leiser R., Pfarrer C., Abd-Elnaeim M. and Dantzer V. (1998). Feto-maternal anchorage in epitheliochorial and endotheliochorial placental types studied by histology and microvascular corrosion casts. Trophoblast Res. 12, 21-39.

Macdonald A.A. and Bosma A.A. (1985). Notes on placentation in the suina. Placenta 6, 83-92.

Macdonald A.A. and Fowden A.L. (1997). Microscopic anatomy of the ungulate placenta. Equine Vet. J. 24, 07-13.

Mayor P., Guimarães D.A., Le Pendu Y., Da Silva J.V., Jori F. and López-Béjar M. (2007). Reproductive performance of captive collared peccaries (*Tayassu tajacu*) in the eastern Amazon. Anim. Reprod. Sci. 102, 88-97.

Mossman H.W. (1987). Vertebrate fetal membranes: comparative ontogeny and morphology, evolution, phylogenic significance, basic functions, research opportunities. Macmillan. London. p 383.

Neudeck H., Unger M., Hufnagl P., Eiben B., Peters K., Kalla J., Graf R. and Vogel M. (1997). Villous cytotrophoblast proliferating potencial in complete or partial hydatidiform mole: diagnostic value of silver-stained nucleolar organizer region (AgNOR)-associated proteins. Gen. Diag. Pathol. 143, 179-184.

Perry J.P. and Crombie R. (1982). Ultrastructure of the uterine glands of the pig. J. Anat. 134, 339-350.

Ploton D., Menager M., Jeannesson P., Himber G., Pigeon F. and Adnet J.J. (1986). Improvement in the staining and in the visualization of the argyrophilic proteins of the nucleolar organizer region at the optical level. Histochem. J. 18, 05-14.

Raub T.J., Bazer F.W. and Roberts R.M. (1985). Localization of the iron transport glycoprotein, uteroferrin, in the porcine endometrium and placenta by using immunocolloidal gold. Anat. Embryol. 171, 253-258.

Renegar R.H., Bazer F.W. and Roberts R.M. (1982). Placental transport and distribution of uteroferrin in the fetal pig. Biol. Reprod. 27, 1247-1260.

Rici R.E.G., Facciotti P.R., Ambrósio C.E., Maria D.A., Kfoury Jr J.R., Bertolini M. and Miglino M.A. (2009). Cell cycle and apoptosis in normal and cloned bovine near-term placentae. Anim. Reprod. Sci. 115, 29-38.

Romao-Correa R.F., Maria D.A., Soma M., Sotto M.N., Sanches J.A. Jr, Neto C.F. and Ruiz I.R. (2005). Nucleolar organizer region staining patterns in paraffin-embedded tissue cells from human skin cancers. J. Cutan. Pathol. 32, 323-328.

Santos T.C., Dantzer V., Oliveira M.F., Jones C.J.P. and Miglino M.A. (2006). Macroscopic and microscopic aspects of collared peccary and white-lipped peccary placenta. Placenta 27, 244-257.

SAS Institute (2001). SAS/STAT User's Guide: Statistics. Ver.8.2, SAS Institute Inc., Cary, NC.

Sinowatz F. and Friess A.E. (1983). Uterine glands of the pig during pregnancy. Anat. Embriol. 166, 121-134.

Smith S. and Sowls L.K. (1975). Fetal development of the collared peccary. J. Mammal. 52, 619-625.

Sowls L.K. (1961). Gestation period of the collared peccary. J. Mammal. 42, 425-426.

Sowls L.K. (1984). The peccaries. University of Arizona Press. Tucson. p 251.

Spencer T.E. and Bazer F.W. (2004). Uterine and placental factors regulating conceptus growth in domestic animals. J. Anim. Sci. 82, E4-E13.

Vallet J.L. and Freking B.A. (2007). Differences in placental structure during gestation associated with large and small pig. J. Anim. Sci. 85, 3267-3275.

Vindelov L.L. and Christensen I.J. (1990). A review of techniques and results obtained in one laboratory by an integrated system of methods designed for routine clinical flow cytometric DNA analysis. Cytometry 11, 753-770.

Zavy M.T, Roberts R.M and Bazer F.W. (1984). Acid phosphatase and leucine aminopeptidase activity in the uterine flushings of non-pregnant and pregnant gilts. J. Reprod. Fertil. 72, 503-507.

Accepted January 13, 2012